IEEE Access
Multidisciplinary ⋮ Rapid Review ⋮ Open Access Journal

Received 9 June 2024, accepted 23 June 2024, date of publication 26 June 2024, date of current version 3 July 2024.

Digital Object Identifier 10.1109/ACCESS.2024.3419147

RESEARCH ARTICLE

Unsupervised Learning-Based Plant Pipeline Leak Detection Using Frequency Spectrum Feature Extraction and Transfer Learning

SUJIN PARK[1], DOYEOB YEO[2], AND JI-HOON BAE[1], (Member, IEEE)
[1]Department of AI and Big Data Engineering, Daegu Catholic University (DCU), Gyeongsan-si 38430, Republic of Korea
[2]Nuclear System Integrity Sensing and Diagnosis Division, Korea Atomic Energy Research Institute (KAERI), Daejeon 34057, Republic of Korea

Corresponding author: Ji-Hoon Bae (jihbae@cu.ac.kr)

This work was supported by the National Research Foundation of Korea through the Government (Ministry of Science and Information and Communications Technology), in 2022, under Grant RS-2022-00165225 and Grant RS-2022-00144000.

ABSTRACT The deterioration of power generation facilities built during the early stages of plant operation is becoming increasingly severe, raising concerns about potential socioeconomic harm from pipe leaks. Consequently, there is a pressing need for rapid leak detection and proactive responses. Prior research primarily relied on various signal processing techniques and supervised learning for leak detection. However, these approaches struggle with accurate detection amid environments with diverse background noises and weak leak signals, exacerbated by challenges in gathering sufficient real-world leakage data, which can lead to overfitting during model learning. Therefore, in this paper, an adaptable leak detection model suitable for various environments was proposed to ensure precise leak detection. Frequency spectrum feature extraction and transfer learning were utilized to achieve accurate leak detection, even with limited data. In addition, an unsupervised learning–based autoencoder model is employed to identify leaks accurately by learning general patterns, even when leakage data is limited. Experimental results demonstrate that the proposed model, integrating feature extraction techniques using the Uniform Manifold Approximation and Projection (UMAP) algorithm and employing transfer learning, achieved a higher accuracy performance with 6.35 percentage points (%p) compared to the model lacking these techniques. In addition, these findings confirm a slight decrease in accuracy performance even when using minimal learning data. Moreover, the leak detection performance was superior to the existing models considered in this study, achieving a high accuracy rate of 99.19%.

INDEX TERMS Pipelines, leak detection, feature extraction, manifold learning, transfer learning, unsupervised learning, autoencoder.

I. INTRODUCTION

The deterioration of power plants and generation facilities constructed during the early stages of operation is accelerating, leading to increased deterioration frequency, and worsening pipe leakage issues.

Pipelines are susceptible to environmental factors such as high temperature, pressure, and humidity, which may result in leakage due to corrosion or various external conditions [1]. Moreover, delayed detection of leaks allows them to expand over time, leading to greater damage. These pipe leaks pose a potential hazard that can lead to safety accidents, economic losses, and environmental pollution issues. Therefore, it is imperative to develop technology for early leak detection and continuous monitoring systems [2], [3].

Currently, there is a growing demand for early leak detection and proactive responses due to aging infrastructure, prompting active research to prevent and minimize damage [4]. In existing studies, data from acoustic or vibration sensors were primarily utilized, employing various signal processing techniques such as time, frequency, and time-frequency domains for leak detection.

The associate editor coordinating the review of this manuscript and approving it for publication was Yongming Li.

However, challenges persist in distinguishing microleaks amid noise and mechanical interference, hindering remote detection [5].

In the era of the Fourth Industrial Revolution, artificial intelligence technology is gaining prominence. In particular, autoencoder (AE) technology, which enables rapid leak detection and real-time response to leaks in industrial settings [6], multilayer perceptron (MLP) [7], deep neural network (DNN) [8], convolutional neural network (CNN) [9], and utilizing machine learning and deep learning models based on recurrent neural network (RNN) [10] are actively researched. Accordingly, this study employed various deep-learning technologies to detect pipe leaks. Moreover, given the challenge of obtaining adequate real-world leakage data [11], this study employed an autoencoder model [12], [13], [14], representative of an unsupervised learning approach [15], to detect leaks by identifying normal data patterns. Furthermore, transfer learning techniques [16], [17] were applied to improve leak detection accuracy across diverse environments with limited data. Thus, this paper proposes an environment-adaptive leak detection model that achieves high accuracy with minimal data based on both unsupervised and transfer learning.

The paper presents several key contributions.

1) The proposed model enhances leakage detection by utilizing the uniform manifold approximation and projection (UMAP) feature extraction algorithm introduced in this study to extract valuable features from the frequency spectrum.
2) An unsupervised learning autoencoder model is proposed to address challenges in collecting adequate leakage data in real environments. This model can detect leaks by learning normal signals from background noise.
3) The transfer learning technique is applied to the autoencoder model mentioned in 2) to mitigate overfitting issues in scenarios with limited training data, ensuring high-accuracy performance across different environments.

This paper's structure is outlined as follows: Chapter II reviews existing literature on leak detection. Chapter III covers data collection and preprocessing and the model proposed in the study. In Chapter IV, experimental results are analyzed, comparing the proposed leak detection model with existing methods. Chapter V presents concluding remarks, summarizing the study's outcomes, and suggesting future research directions.

II. RELATED WORK

Before the advent of artificial intelligence technology, leak detection relied on traditional signal processing techniques. Wang et al. [18] proposed an acoustic-based method employing time-domain statistical feature extraction. Lee et al. [19] introduced a leak detection technique involving injecting fluid transients into a pipeline, followed by the analysis of the resulting transient trace in the frequency domain. Furthermore, Yao et al. [20] presented a time-frequency analysis-based method for hydraulic actuator leak detection. In a related context, Ferrante et al. [21] employed harmonic analysis and wavelet analysis for efficient pressure signal analysis and leak localization. These techniques, adopted as primary signal processing methods, were mainly conducted in the early stages of leakage detection research. However, these methods faced challenges in accurately detecting leaks in noisy environments.

To overcome these limitations, research focuses on enhancing leakage detection accuracy using artificial intelligence. Bae et al. [22] generated root mean square (RMS) patterns in the time domain and frequency pattern image features in the frequency domain. These patterns were subsequently employed in training a convolutional neural network (CNN)-based artificial intelligence model. The aim was to detect stable pipe leaks in noisy environments featuring complex machine operations. Experimental results substantiated the achievement of satisfactory performance. Mandal et al. [23] proposed a leak detection technique based on rough set theory and support vector machine (SVM) algorithm to reduce false leak detection. Mashhadi et al. [24] evaluated six machine learning methods for leak location identification in water distribution systems (WDS), with logistic regression and random forest showing excellent performance. Chuang et al. [25] introduced an acoustic leak detection approach using a CNN with Mel frequency cepstrum coefficients for groundwater pipelines.

Furthermore, Yang et al. [26] proposed a Pressure Point Analysis (PPA) leak detection method based on a Supervised Optimally-Pruned Extreme Learning Machine (OPELM) coupled with a bidirectional recurrent neural network for continuous pressure monitoring. These studies represent notable deep learning–based approaches, predominantly employing supervised learning [27]. Whereas supervised learning methods have demonstrated high accuracy in leak detection even in noisy environments, challenges arise in collecting sufficient leak data in real-world settings, potentially affecting deep learning model training.

To address this, leak detection research using an unsupervised learning method that can detect leaks by learning normal data is being introduced. Moreover, it is widely used for anomaly detection in various fields, including cybersecurity, financial fraud detection, and medical equipment anomaly detection. It identifies leaks by learning normal patterns without an answer key. Typical examples include autoencoder [28] and clustering [29], and autoencoder models are primarily used in time series data. An autoencoder consists of an encoder [30] and a decoder [31]. This architecture is designed to compress input data at the encoder and reconstruct it at the decoder to reinterpret the initial input. This structural design aims to enhance detection accuracy and holds the advantage of effectively capturing nonlinear relationships [32].

Transfer learning, alongside unsupervised learning, has garnered attention for transferring knowledge from a source domain to improve the learning performance in a target domain [33]. This facilitates efficient knowledge learning in the target domain environment, enabling high-accuracy performance even with limited data. Moreover, research combined with unsupervised learning is in progress [34], [35], which allows rapid and effective learning of new tasks. Therefore, this study aims to achieve high-accuracy leak detection in various environments by utilizing signal processing techniques and deep learning technology. To this end, the study adopts an autoencoder, an unsupervised learning technique, as the model structure based on transfer learning. Given the vulnerability of time domain signals to external noise environments, only frequency domain characteristics are considered. The following sections describe the data utilized and comprehensively describe the proposed pipe leak detection model.

III. PROPOSED METHOD

This section outlines the data collection and preprocessing for implementing an environmentally adaptive leak detection model. In addition, a detailed description of the proposed model, based on transfer learning and unsupervised learning, is provided.

A. DATA COLLECTION AND FEATURE EXTRACTION PREPROCESSING

For the implementation of an environment-adaptive leak detection model, noise and leak data were collected from two different environments. The target domain refers to the environment where the leak detection model will be applied, whereas the source domain provides knowledge for transfer to the target domain. Noise data, obtained by measuring various mechanical noises around pipes, represents steady-state data typical in living environments. Normal and leakage time series data were collected from both domains using four microphone acoustic sensors installed on a plant piping system testbed, as shown in Figure 1 [36].

In the source domain environment, normal and leakage data were initially collected at a sampling frequency of 100 kHz for each channel. Leakage data was measured at 100 locations of leaky pipes. A total of 25 combinations comprising 5 types of leakage pressure (1, 2, 3, 4, 5 bar) and 5 types of leakage size (0.5, 1.0, 1.5, 2.0, 2.5 mm) were created to collect a diverse range of leakage data, including microleakage conditions. Moreover, 450,000 leakage data points were collected for each sensor.

Subsequently, in the target domain environment, normal and leakage data were collected at a sampling frequency of 100 kHz for each channel, with leakage data measured at eight locations of leaky pipes. Low-level leak data were gathered with a leak size set to 0.5 mm, and leak pressure varied from 1 to 2 bar, resulting in 500,000 leak data points per sensor.

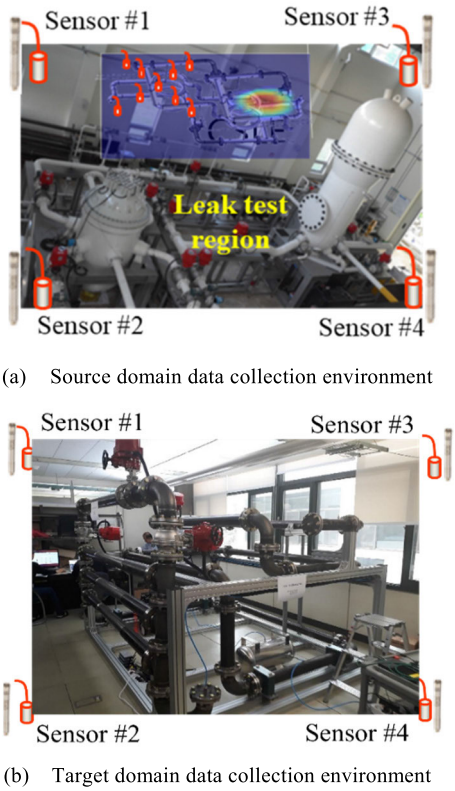

FIGURE 1. Data collection environment for implementing the proposed leak detection model using transfer learning.

B. FREQUENCY FEATURE EXTRACTION PREPROCESSING

This section aims to extract useful information from raw data collected through measurements by utilizing signal characteristics in the frequency domain. Although signal analysis in the time domain can also be applied for leak detection in this study, approaches utilizing amplitude information in the time domain are generally easily affected by background noise and surrounding mechanical noise, which can degrade detection performance. In addition, given the commercial availability of leak detection devices that utilize filtering and spectral signal processing analysis in specific sections of the frequency domain, this study considers feature extraction preprocessing in the frequency domain rather than the time domain. Figure 2 illustrates the application of the frequency feature extraction signal processing to both normal and leaky sample data collected in the testbed depicted in Figure 1. Initially, the sampled data underwent low-pass filtering (LPF) [37] to retain frequencies below 45 KHz. Subsequently, a band-pass filter (BPF) was applied to extract the specific band where the leakage signal is distributed (set to 4 kHz to 45 kHz in this study), aiming to eliminate background noise [38]. After applying these filters, the Fourier transform (FT) was then applied to the normal and leakage data using equation (1), with the result converted to a frequency domain spectrum signal using the absolute value function [39].

$$\mathrm{FT} = \left| \int_{-\infty}^{\infty} s_t \cdot e^{-j2\pi st} dt \right|, \tag{1}$$

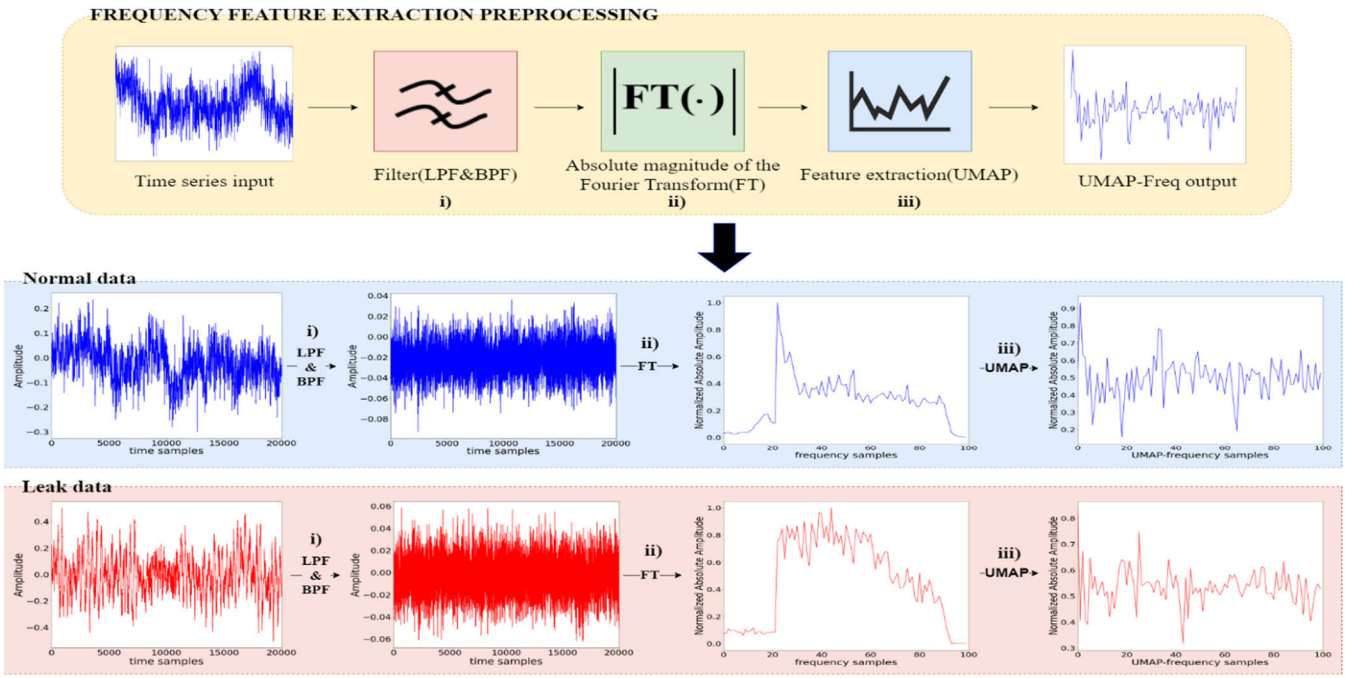

FIGURE 2. Data signal processing for frequency feature extraction.

where s_t refers to the time domain input signal and $e^{-j2\pi st}$ represents the complex exponential function corresponding to each frequency component in the frequency domain. Next, to reduce the computational workload and simplify the complexity required for model learning, the signal output in (1) was divided into 100 sections, where the average value of the spectral sample magnitude for each section is calculated as a representative value, resulting in a spectrum magnitude vector with 100 frequency samples. Therefore, through appropriate signal filtering, including (1), as shown in Figure 2, observing the maximum magnitude and spectral shape differences between normal and leaky signals within a specified frequency range is possible.

Lastly, the data preprocessing techniques for extracting key features from the frequency spectrum magnitude vectors involve the UMAP algorithm [40]. The UMAP algorithm is a nonlinear neighborhood graph-based algorithm, and calculations are made through the construction of a specific weighted k-neighbor graph. This algorithm attempts to preserve the dataset's local environment rather than preserving its large-scale structure by assigning higher weights to closer neighbors. Therefore, it operates by identifying a preset number of nearest neighbors and assigning more weight to the nearest neighbors based on their distance [41]. The application of the UMAP algorithm is illustrated by equation (2).

$$\text{UMAP} = \exp\left(-\frac{d(\text{FT}(a)\text{FT}(b))^2}{\sigma_a \sigma_b}\right), \tag{2}$$

where $d(\text{FT}(a)\text{FT}(b))$ refers to the distance between data points, a and b, and $\sigma_a\sigma_b$ refers to the Gaussian kernel widths. The position of the data is measured through Euclidean distance calculation and squaring the result, quickly reducing the weight of the distance between distant data points. In addition, dividing the value by the Gaussian kernel width properly adjusts weights and distances between data points.

The UMAP algorithm generally focuses on very local structures when the number of neighbors is small. When it is large, it forces the user to look at larger neighbors of each point when estimating various data structures [42]. In this study, Euclidean distance was used to measure distance, and the number of neighbors was set to five. This value was selected experimentally and set to the small neighborhood's value to preserve the local structure. The results obtained by applying the UMAP algorithms to the frequency spectrum magnitude vector are defined as the UMAP-Freq feature (UMAP). Therefore, in this study, a feature extraction algorithm is applied to the frequency spectrum magnitude vector, as depicted in Figure 2, and the resulting feature vector is utilized for model learning.

C. AUTOENCODER-BASED LEAK DETECTION MODEL USING TRANSFER LEARNING

This section presents an autoencoder-based leak detection model applicable to various environments through transfer learning. The proposed process structure, as shown in Figure 3, undergoes a two-stage model learning process (Stage 1, Stage 2) and a leak detection phase. As the stage progresses from Stage 1 to Stage 2, transfer learning is

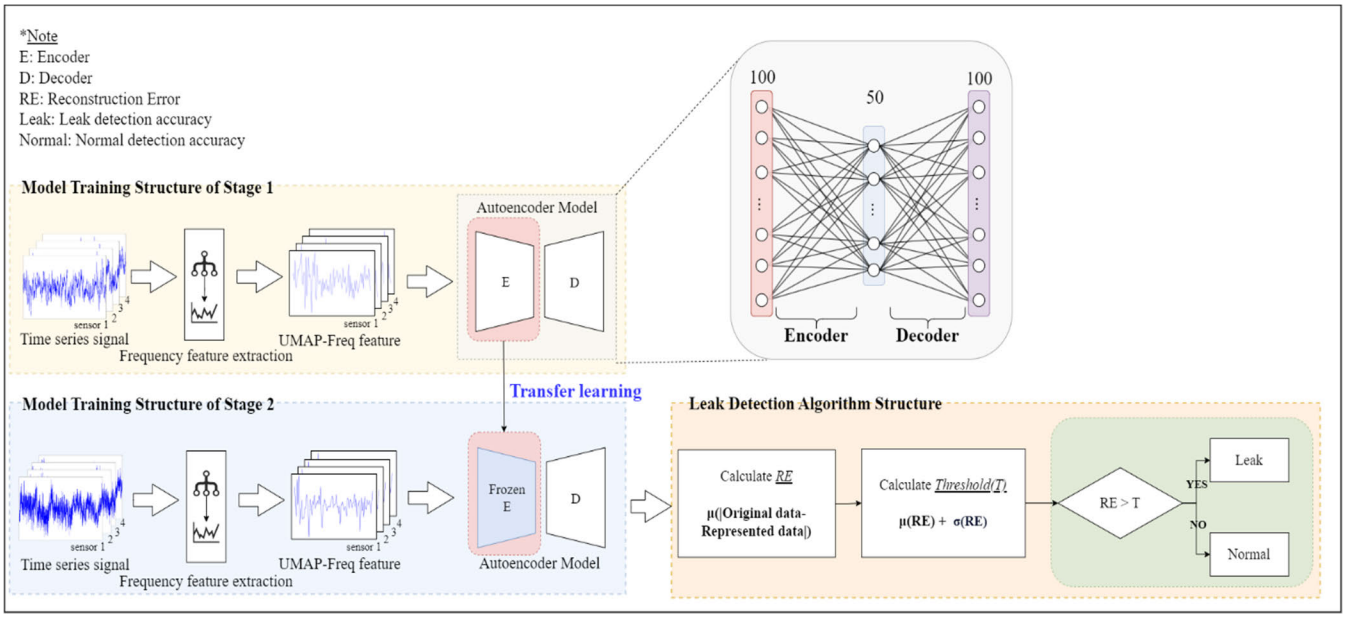

FIGURE 3. Proposed model architecture for leak detection.

applied. Stage 1, the initial step in the proposed model, utilizes source domain data and undergoes the frequency feature extraction processing, as illustrated in Figure 2. Specifically, the UMAP-Freq feature data extracted from the source domain data through (1) and (2) serves as input for the unsupervised learning–based autoencoder model presented in (3) and (4). The model is trained solely on normal data, excluding leakage instances.

$$z = W_{encoder} \cdot x + b_{encoder}, \tag{3}$$

$$\bar{x} = W_{decoder} \cdot z + b_{decoder}, \tag{4}$$

where $W_{encoder}$ refers to the encoder's weight matrix, x refers to the input data, and $b_{encoder}$ refers to the encoder's bias vector. Equation (3) produces the latent expression "z," used in the decoder computation. Moreover, $W_{decoder}$ in (4) denotes the decoder's weight matrix, and $b_{decoder}$ presents the decoder's bias vector. The decoder is computed using the latent vector calculated in the encoder, resulting in the output of $\bar{x}$, the reconstructed value for the input data. In this study, four autoencoder series model structures are considered, including multilayer perceptron (MLP), deep neural network (DNN), one-dimensional convolutional neural network (1D CNN), and separable one-dimensional convolutional neural network (Separable 1D CNN). MLP and DNN handle two-dimensional input data through a fully connected neural network, adjusting weights between neurons in each layer. Conversely, 1D CNN and Separable 1D CNN operate on three-dimensional input data, utilizing 1D convolution and depth-wise separable convolution operations for feature extraction from the input data. In Chapter 4, the leak detection accuracy performance of the four models described above are compared. Upon completing Stage 1 learning, the encoder model is saved and transferred to Stage 2 for incremental transfer learning.

Stage 2 utilizes target domain data, applying the same frequency feature extraction processing techniques as Stage 1. To utilize source domain knowledge, the weights of the pretrained encoder model from Stage 1 are frozen, and the decoder model is applied to perform retraining.

Upon completing Stage 2 learning, the leak detection algorithm is executed to determine leak presence, as depicted in the "Leak detection algorithm block" in Figure 3. Initially, the reconstruction error is computed by calculating the difference between the encoder input signal and the decoder output signal, as expressed in equation (5).

$$\mathrm{RE} = \frac{1}{N} \sum_{i=1}^{N} |x - \bar{x}|, \tag{5}$$

where N refers to the number of data samples, x refers to the input signal, and $\bar{x}$ refers to the reconstruction signal output through the decoder. The calculated reconstruction error value is used to set the threshold (T), and the abnormality detection threshold for normal signals is calculated as in equation (6).

$$T = \mu\,(\mathrm{RE}) + \sigma\,(\mathrm{RE})\,, \tag{6}$$

where $\mu(\cdot)$ denotes the average, $\sigma(\cdot)$ denotes the standard deviation, and RE denotes the reconstruction error in (5). The presence of leaks is determined using the model created through step-by-step transfer learning of Stage 1 and Stage 2. This determination relies on the sum of the mean (μ) and standard deviation (σ) for RE. A threshold is established with the combined value, set within the range where a normal signal exists, and calculated using the reconstruction error

Algorithm 1 Overall Procedure for the Leak Detection Process Based on Transfer Learning and Unsupervised Learning

•Stage 1: By applying the frequency feature extraction technique, an unsupervised learning-based autoencoder model is learned.

1) Time series data from the source domain is converted into a frequency spectrum magnitude signal, as depicted in the "Model Training Structure of Stage 1 block" in Figure 3. Subsequently, the UMAP-Freq feature is extracted using (2).

2) Based on the extracted UMAP-Freq feature data, an autoencoder model utilizing an artificial neural network–based structure is trained.

•Stage 2: The transfer learning technique is utilized to implement a leak detection model in the target domain by transferring the pre-trained encoder from Stage 1.

1) Time series data from the target domain is converted into a frequency spectrum magnitude signal, as shown in the "Model Training Structure of Stage 2 block" in Figure 3. Subsequently, the UMAP-Freq feature is extracted using (2).

2) Using the extracted UMAP-Freq feature data, the weights of the encoder model obtained in Stage 1 are frozen, and the decoder model is additionally applied to perform retraining.

•Leak detection phase: Utilizing the autoencoder model with transfer learning completed from Stage 1 to Stage 2, leakage is determined by establishing a threshold based on the reconstruction error.

1) As depicted in the "Leak detection algorithm block" in Figure 3, the threshold is determined from (6) based on the reconstruction error value.

2) Based on the set threshold, the presence of leakage in the new input signal is determined.

values of normal data through (6). Normal and leak states are determined based on this threshold: if the reconstruction error value exceeds the threshold, it is identified as a leak; if it is below the threshold, it is classified as normal.

An overview of the leak detection technique, applying transfer learning and unsupervised learning as proposed in this study, is outlined in Algorithm 1, which is then utilized to compare the performance of leak detection based on data feature extraction and transfer learning.

IV. EXPERIMENT RESULTS

Chapter 4 comprises three sections, outlined as follows. First, Section IV-A evaluates leak detection performance with and without the feature extraction technique. In Section IV-B, we assess leak detection performance with and without the transfer learning technique, also examining performance changes based on the training data utilization ratio. Lastly, in Section IV-C, we conclude by comparing the leak detection performance of the proposed model against an existing supervised learning model.

A. LEAK DETECTION PERFORMANCE OF THE PROPOSED MODEL USING FREQUENCY FEATURE EXTRACTION

In this section, leak detection performance is assessed by exclusively training Stage 2 of the model structure depicted in Figure 3. This evaluation focuses on the application of feature extraction techniques, namely the UMAP algorithm, to the frequency spectrum data. Notably, transfer learning is excluded, and Stage 1 is not considered. Leak detection performance is compared between unsupervised learning–based autoencoder models across four neural network structures, including MLP, DNN, 1D CNN, and Separable 1D CNN.

To train the model, 7,500 pieces of normal data were randomly sampled for each sensor from the target domain data, totaling 30,000 pieces of data. These were divided into a 2:1 ratio composed of 20,000 training data and 10,000 test data. In addition, 10,000 test data points were extracted from the leak data in the target domain for executing the leak detection algorithm. Ultimately, 20,000 test data points representing both normal and leak scenarios were utilized.

The four autoencoder models implemented for leak detection were categorized into two-dimensional input-based models (MLP and DNN) and three-dimensional input-based models (1D CNN and Separable 1D CNN). The structures of each model are detailed in Tables 1 to 4.

TABLE 1. Detailed structure of autoencoder model based on MLP structure.

Model information	Layer information	Number of neurons	Param
Encoder	Input	100	0
Latent Layer	Dense	50	5,050
Decoder	Dense	100	5,100
*Total params		10,150	

TABLE 2. Detailed structure of autoencoder model based on DNN structure.

Model information	Layer information	Number of neurons	Param
Encoder	Input	100	0
	Dense	80	8,080
	Dense	50	4,050
Latent layer	Dense	30	1,530
Decoder	Dense	50	1,550
	Dense	80	4,080
	Dense	100	8,100
*Total params		27,390	

In the notation, Dense denotes a fully connected layer, Conv1d denotes a 1D convolution layer, Separable Conv1d

TABLE 3. Detailed structure of autoencoder model based on 1D CNN structure.

Model information	Layer information	Length of timesteps	Number of features	Param
Encoder	Input	100	1	0
	Conv1d	100	8	32
	Maxpooling1d	50	8	0
	Conv1d	50	16	400
Latent layer	Maxpooling1d	25	16	0
Decoder	Conv1d	25	16	784
	Upsampling1d	50	16	0
	Conv1d	50	8	136
	Upsampling1d	100	8	0
	Conv1d	100	1	25
*Total params			1,377	

TABLE 4. Detailed structure of autoencoder model based on separable 1D CNN structure.

Model information	Layer information	Length of timesteps	Number of features	Param
Encoder	Input	100	1	0
	Separable Conv1d	100	8	19
	Maxpooling1d	50	8	0
	Separable Conv1d	50	16	168
Latent layer	Maxpooling1d	25	16	0
Decoder	Separable Conv1d	25	16	320
	Upsampling1d	50	16	0
	Separable Conv1d	50	8	184
	Upsampling1d	100	8	0
	Separable Conv1d	100	1	33
*Total params			724	

for a 1D depth-separating convolution layer, Maxpooling1d for a 1D maximum pooling layer, and Upsampling1d denotes a data dimension expansion layer.

Learning parameters suitable for the four models were determined using validation data, setting the learning rate to 0.001 with the RMSprop learning algorithm [43]. The number of learning epochs and batch size were determined based on the model structure. For the 2D input-based model, the number of epochs was set to 30, with a batch size of 32. For the 3D input-based model, the number of epochs was set to 50, with a batch size of 64. The loss function was set to mean squared error (MSE) because all four models were regression models using unsupervised learning, and the performance evaluation metric was set to mean absolute error (MAE).

The performance comparison of the four models, along with the results of leak detection performance measurements based on the application of the UMAP extraction algorithm, is presented in Table 5. Through the test methodology of three-fold cross-validation, each model underwent a total of five learning sessions, with leak detection performance described based on the average of the measured values. UMAP-Freq represents features extracted by applying the UMAP algorithm. Analysis of the experimental results in Table 5 indicates that models applying the feature extraction technique outperformed those that did not.

TABLE 5. Leak detection accuracy (%) by autoencoder models depending on the application of feature extraction technique.

Model/ Data Type	MLP	DNN	1D CNN	Separable 1D CNN
Freq	92.84	88.83	86.26	88.78
UMAP-Freq	**98.83**	97.54	95.89	98.10

Furthermore, another feature extraction method, principal component analysis (PCA) [44], [45], was considered for comparison with UMAP, as shown in Figure 4. The notation PCA-Freq represents features extracted by applying the PCA algorithm to the frequency spectrum magnitude signal (Freq). The output feature dimension using PCA and UMAP was set to match the original frequency spectrum size vector dimension for comparison purposes. Notably, the UMAP algorithm showed superior performance compared to PCA. In addition, Table 5 and Figure 4 illustrate that among the models utilizing the UMAP algorithm, the MLP model exhibited the highest leak detection performance, achieving 98.83% accuracy.

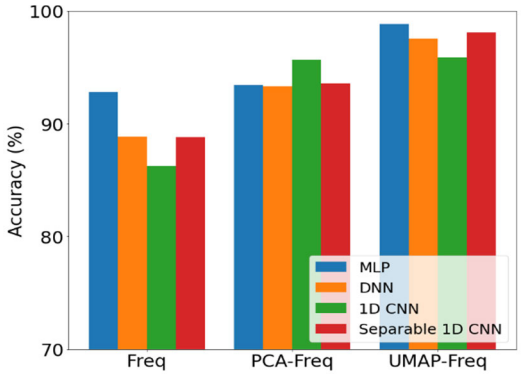

FIGURE 4. Comparison of leak detection model performance based on the application of feature extraction techniques.

Furthermore, the autoencoder model based on the MLP structure with UMAP-Freq features demonstrated excellent signal restoration performance, as shown in Figure 5.

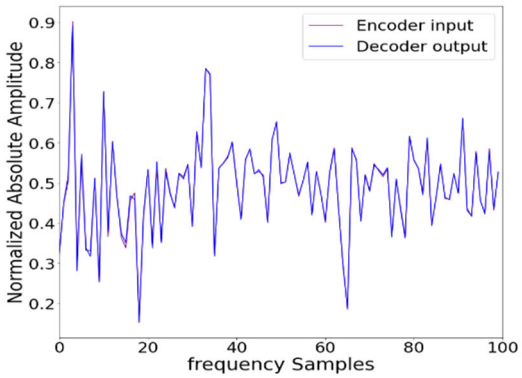

FIGURE 5. Signal restoration results of an autoencoder model based on the MLP structure applying UMAP-Freq features.

B. LEAK DETECTION PERFORMANCE DEPENDING ON TRANSFER LEARNING TECHNIQUE APPLICATION

This section presents a comparison of the leak detection performance of an MLP-structured autoencoder model utilizing the UMAP-Freq feature, which showed the best performance in Section IV-A. The comparison is based on whether the transfer learning technique presented in Figure 3 is applied. For models without transfer learning techniques, only the "Model Training Structure of Stage 2 block" is performed in Figure 3, defining this as the base model.

First, Table 6 presents the experimental result evaluating the impact of applying the UMAP algorithm in the proposed method for transfer learning. The objective of this experiment is to evaluate leak detection performance using the original frequency spectrum data and UMAP-Freq feature data under the same transfer learning condition. Through this analysis, we aim to quantify the degree of performance enhancement resulting from the application of the UMAP algorithm. Analysis of the experimental result in Table 6 indicates that the application of the UMAP algorithm in transfer learning yielded the best performance. This represents a 6.02 %p improvement compared to the transfer learning model without the UMAP algorithm.

TABLE 6. Leak detection accuracy (%) depending on the application of UMAP to the proposed model with transfer learning.

Data Type	Accuracy (%)	Reference
Freq	93.17	With TL
UMAP-Freq	**99.19**	With TL

Next, leak detection performance, depending on the application of transfer learning techniques, is provided in Table 7. In this study, to investigate changes in leak detection performance with decreasing training data utilization ratios, the number of test data was fixed at 10,000. The training data was systematically reduced to 100%, 70%, 50%, 30%, 10%, and 5% of its original size, and accuracy was measured for each ratio. Here, the model's performance was evaluated using three-fold cross-validation.

TABLE 7. Leak detection accuracy (%) based on training data utilization ratio.

Model / Train data rate (%)	Base model	Transfer learning–based model	Performance improvement
100	98.83	**99.19**	0.36%p ↑
70	98.75	99.13	0.38%p ↑
50	98.05	98.89	0.84%p ↑
30	97.72	98.77	1.05%p ↑
10	97.03	98.69	1.66%p ↑
5	93.87	98.58	4.71%p ↑

The performance measurement results of the proposed model using both the base model and transfer learning technique across different training data utilization ratios are presented in Table 7 and Figure 6. Analyzing Table 7 reveals that the model's accuracy performance with the applied transfer learning technique remains relatively stable, even with reduced training data, whereas the model without transfer learning shows a noticeable decrease in accuracy as the training data decreases. Specifically, the proposed model achieves a higher accuracy performance with 0.36 percentage points (%p) compared to the base model without transfer learning, based on 100% training data utilization. This performance gap widens as the training data utilization ratio decreases, as quantitatively shown in Table 7 and Figure 6.

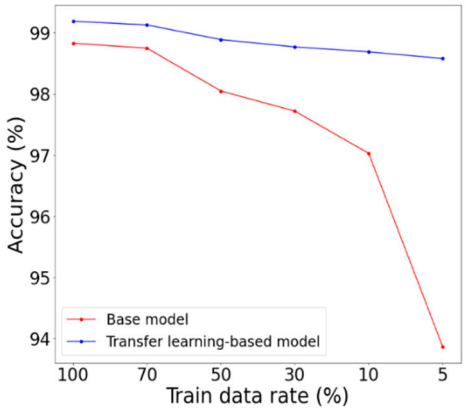

FIGURE 6. Comparison of leak detection model performance according to training data utilization ratio.

C. COMPARISON WITH EXISTING SUPERVISED LEARNING MODEL

This section presents a comparison of the leak detection performance of existing supervised machine learning models with the proposed model. Models such as 1D CNN, logistic regression, long short-term memory (LSTM), and SVM were considered supervised learning leak detection models. Performance comparison was conducted using

various training data ratios, where "Train data rate (%)" in Table 8 and Figure 7 represents the utilization rates of the training data at 100%, 70%, 50%, 30%, and 1%. The model's performance was evaluated using a three-fold cross-validation test methodology. Binary Crossentropy was selected as the loss function because of the binary label setup in supervised learning. In addition, leak detection performance was evaluated using the same data configuration as the proposed model, allowing frequency spectrum size data from the target domain to be input into the supervised learning model.

TABLE 8. Leak detection accuracy (%) performance comparison between the proposed model and a supervised learning–based model.

Train data rate (%) / Model	100	70	50	30	1
1D CNN	92.37	90.34	88.43	72.04	60.96
Logistic Regression	83	82	81	76	72
LSTM	81.05	80	79	65	53
SVM	86	84	82	68	54
Proposed model	**99.19**	99.13	98.89	98.77	98.14

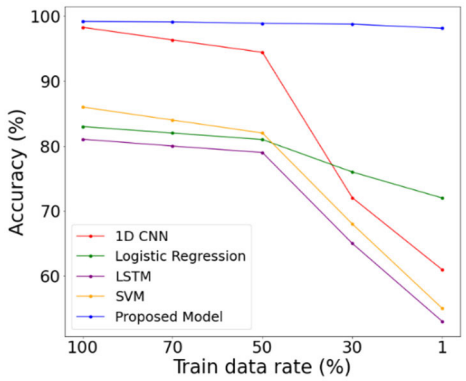

FIGURE 7. Results of leak detection accuracy performance comparison according to training data utilization ratio.

Analysis of the experimental results in Table 8 and Figure 7 indicates that the proposed model exhibited superior leak detection performance, achieving an accuracy of 99.19%. Furthermore, whereas the accuracy of the existing models based on supervised learning notably decreases with reduced training data, the proposed model shows minimal performance degradation. Leveraging transfer learning, where the pretrained encoder model from Stage 1 is utilized for step-by-step learning, the proposed model consistently demonstrates high-accuracy performance, reaching 98.14% accuracy even with limited training data.

In addition, confusion matrix–based performance measurements of precision, recall, and F1-score demonstrate that the proposed model outperforms existing models, as shown in Table 9. Precision refers to the proportion of cases predicted as leaks by the model that are actually leaks. Recall refers to the proportion of actual leak cases that the model correctly predicts as leaks. F1-score is the harmonic mean of precision and recall, effectively distinguishing between leaks and normal cases and ensuring a good balance between precision and recall. Analysis of the experimental results in Table 9 indicates that the proposed model shows superior precision, recall, and F1-score compared to the existing models. This represents a significant improvement in leak and normal detection accuracy compared to previous research models.

TABLE 9. Leak detection performance (%) results using the precision, recall, and F1-score performance metrics.

Performance / Model	Precision	Recall	F1-score
1D CNN	88.24	97.78	92.37
Logistic Regression	75.41	97.36	84.99
LSTM	98.61	95.68	97.12
SVM	78.85	98.08	87.42
Proposed model	100	98.39	99.19

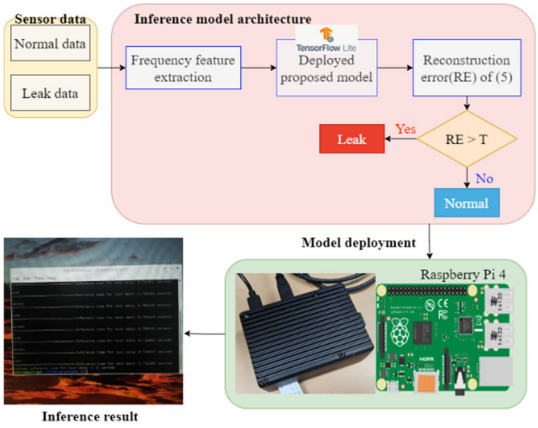

FIGURE 8. Experimental environment for inference on the proposed model deployed on Raspberry Pi 4.

Finally, we performed an inference experiment by deploying the leak detection model—after completing the proposed stagewise transfer learning for the MLP-based autoencoder—onto a lightweight embedding board, as shown in Figure 8. We converted the proposed model into a lightweight version using TensorFlow Lite [46] for deployment on the Raspberry Pi. Inference performance was measured by the time taken to distinguish between leaks and normal conditions after preprocessing the data through frequency feature extraction. The proposed model's performance was evaluated using a total of 20 mixed datasets, consisting of 10 normal instances and 10 leak instances, with the inference results shown in Figure 8. The average inference time for 20 consecutive normal and leak data instances was 0.72 s. This

experimental result indicates that the proposed method can perform reasonably fast inference within 1 s, meeting the required operational runtime despite the constraints of limited computing resources.

V. CONCLUSION

In this study, an unsupervised learning–based leakage detection model using a transfer learning technique designed for versatility across various environments was proposed. By applying the transfer learning technique, which leverages knowledge gained from the source domain to enhance learning in the target domain, the proposed model demonstrated experimentally high accuracy in leak detection performance, even with limited training data. In addition, employing unsupervised learning autoencoder models aids in leak identification by learning background noise patterns, which is particularly beneficial in scenarios with limited leak data. The proposed model works by initially learning to interpret data patterns through an encoder that compresses the input data and a decoder that reconstructs it. The reconstruction error, which is the difference between the original input and the reconstructed output, helps define a threshold for determining normal and leak states: reconstruction error values above this threshold indicate leaks, while those below are classified as normal. Furthermore, applying the UMAP algorithm to frequency spectrum signals enhances the model's performance by utilizing meaningful data information.

Moving forward, leveraging the model proposed in this study, we aim to explore the development of a continuous monitoring system capable of providing real-time feedback on countermeasures to mitigate issues through constant surveillance. Furthermore, based on this study's successful application experiments on transfer learning from a source domain emulating the actual environment to a target domain, we plan to conduct future experiments to assess model transfer reliability and generalization. These experiments will involve applying the proposed approach to real-world leakage detection and extending the research to include a deeper investigation of data distributions for leak detection beyond the distance-based threshold technique considered in this study.

REFERENCES

[1] N. V. S. Korlapati, F. Khan, Q. Noor, S. Mirza, and S. Vaddiraju, "Review and analysis of pipeline leak detection methods," *J. Pipeline Sci. Eng.*, vol. 2, no. 4, Dec. 2022, Art. no. 100074, doi: 10.1016/j.jpse.2022.100074.

[2] A. Nasirian, M. F. Maghrebi, and S. Yazdani, "Leakage detection in water distribution network based on a new heuristic genetic algorithm model," *J. Water Resource Protection*, vol. 5, no. 3, pp. 294–303, Mar. 2013, doi: 10.4236/jwarp.2013.53030.

[3] H. Ali and J.-H. Choi, "A review of underground pipeline leakage and sinkhole monitoring methods based on wireless sensor networking," *Sustainability*, vol. 11, no. 15, p. 4007, Jul. 2019, doi: 10.3390/su11154007.

[4] S. El-Zahab and T. Zayed, "Leak detection in water distribution networks: An introductory overview," *Smart Water*, vol. 4, no. 1, p. 5, Jun. 2019, doi: 10.1186/s40713-019-0017-x.

[5] D. Yeo, J.-H. Bae, and J.-C. Lee, "Unsupervised learning-based pipe leak detection using deep auto-encoder," *J. Korea Soc. Comput. Inf.*, vol. 24, no. 9, pp. 21–27, Sep. 2019, doi: 10.9708/jksci.2019.24.09.021.

[6] T. T. N. Luong and J.-M. Kim, "The enhancement of leak detection performance for water pipelines through the renovation of training data," *Sensors*, vol. 20, no. 9, p. 2542, Apr. 2020, doi: 10.3390/s20092542.

[7] A. Pinkus, "Approximation theory of the MLP model in neural networks," *Acta Numerica*, vol. 8, pp. 143–195, Jan. 1999, doi: 10.1017/s0962492900002919.

[8] B. Zhou, V. Lau, and X. Wang, "Machine-learning-based leakage-event identification for smart water supply systems," *IEEE Internet Things J.*, vol. 7, no. 3, pp. 2277–2292, Mar. 2020, doi: 10.1109/JIOT.2019.2958920.

[9] T. Kattenborn, J. Leitloff, F. Schiefer, and S. Hinz, "Review on convolutional neural networks (CNN) in vegetation remote sensing," *ISPRS J. Photogramm. Remote Sens.*, vol. 173, pp. 24–49, Mar. 2021, doi: 10.1016/j.isprsjprs.2020.12.010.

[10] W. Yin, K. Kann, M. Yu, and H. Schütze, "Comparative study of CNN and RNN for natural language processing," 2017, *arXiv:1702.01923*.

[11] R. A. Cody, B. A. Tolson, and J. Orchard, "Detecting leaks in water distribution pipes using a deep autoencoder and hydroacoustic spectrograms," *J. Comput. Civil Eng.*, vol. 34, no. 2, Mar. 2020, Art. no. 04020001, doi: 10.1061/(asce)cp.1943-5487.0000881.

[12] M. Tschannen, O. Bachem, and M. Lucic, "Recent advances in autoencoder-based representation learning," 2018, *arXiv:1812.05069*.

[13] C.-Y. Liou, W.-C. Cheng, J.-W. Liou, and D.-R. Liou, "Autoencoder for words," *Neurocomputing*, vol. 139, pp. 84–96, Sep. 2014, doi: 10.1016/j.neucom.2013.09.055.

[14] D. Bank, N. Koenigstein, and R. Giryes, "Autoencoders," in *Machine Learning for Data Science Handbook*. Cham, Switzerland: Springer, 2023, pp. 353–374, doi: 10.1007/978-3-031-24628-9_16.

[15] H. B. Barlow, "Unsupervised learning," *Neural Comput.*, vol. 1, no. 3, pp. 295–311, Sep. 1989, doi: 10.1162/neco.1989.1.3.295.

[16] L. Torrey and J. Shavlik, "Transfer learning," in *Handbook of Research on Machine Learning Applications and Trends: Algorithms, Methods, and Techniques*, E. S. Olivas, Ed. Hershey, PA, USA: IGI Global, 2010, pp. 242–264, doi: 10.4018/978-1-60566-766-9.ch011.

[17] S. Niu, Y. Liu, J. Wang, and H. Song, "A decade survey of transfer learning (2010–2020)," *IEEE Trans. Artif. Intell.*, vol. 1, no. 2, pp. 151–166, Oct. 2020, doi: 10.1109/TAI.2021.3054609.

[18] F. Wang, W. Lin, Z. Liu, S. Wu, and X. Qiu, "Pipeline leak detection by using time-domain statistical features," *IEEE Sensors J.*, vol. 17, no. 19, pp. 6431–6442, Oct. 2017, doi: 10.1109/JSEN.2017.2740220.

[19] P. J. Lee, J. P. Vítkovský, M. F. Lambert, A. R. Simpson, and J. A. Liggett, "Frequency domain analysis for detecting pipeline leaks," *J. Hydraulic Eng.*, vol. 131, no. 7, pp. 596–604, Jul. 2005, doi: 10.1061/(ASCE)0733-9429(2005)131:7(596).

[20] Z. Yao, J. Tang, T. Rui, and J. Duan, "A time–frequency analysis based internal leakage detection method for hydraulic actuators," *Adv. Mech. Eng.*, vol. 9, no. 1, pp. 1–8, Jan. 2017, doi: 10.1177/1687814016685058.

[21] M. Ferrante, B. Brunone, and S. Meniconi, "Wavelets for the analysis of transient pressure signals for leak detection," *J. Hydraulic Eng.*, vol. 133, no. 11, pp. 1274–1282, Nov. 2007, doi: 10.1061/(ASCE)0733-9429(2007)133:11(1274).

[22] J.-H. Bae, D. Yeo, D. B. Yoon, S. W. Oh, G. J. Kim, N. S. Kim, and C. S. Pyo, "Deep-learning-based pipe leak detection using image-based leak features," in *Proc. 25th IEEE Int. Conf. Image Process. (ICIP)*, Athens, Greece, Oct. 2018, pp. 2361–2365, doi: 10.1109/ICIP.2018.8451489.

[23] S. K. Mandal, F. T. S. Chan, and M. K. Tiwari, "Leak detection of pipeline: An integrated approach of rough set theory and artificial bee colony trained SVM," *Exp. Syst. Appl.*, vol. 39, no. 3, pp. 3071–3080, Feb. 2012, doi: 10.1016/j.eswa.2011.08.170.

[24] N. Mashhadi, I. Shahrour, N. Attoue, J. El Khattabi, and A. Aljer, "Use of machine learning for leak detection and localization in water distribution systems," *Smart Cities*, vol. 4, no. 4, pp. 1293–1315, Oct. 2021, doi: 10.3390/smartcities4040069.

[25] W.-Y. Chuang, Y.-L. Tsai, and L.-H. Wang, "Leak detection in water distribution pipes based on CNN with mel frequency cepstral coefficients," in *Proc. 3rd Int. Conf. Innov. Artif. Intell.*, Suzhou, China, Mar. 2019, pp. 83–86, doi: 10.1145/3319921.3319926.

[26] L. Yang and Q. Zhao, "A novel PPA method for fluid pipeline leak detection based on OPELM and bidirectional LSTM," *IEEE Access*, vol. 8, pp. 107185–107199, 2020, doi: 10.1109/ACCESS.2020.3000960.

[27] P. Cunningham, M. Cord, and S. J. Delany, "Supervised learning," in *Machine Learning Techniques for Multimedia. Cognitive Technologies*. Berlin, Germany: Springer, 2008, doi: 10.1007/978-3-540-75171-7_2.

[28] M. Kammoun, A. Kammoun, and M. Abid, "LSTM-AE-WLDL: Unsupervised LSTM auto-encoders for leak detection and location in water distribution networks," *Water Resour. Manag.*, vol. 37, no. 2, pp. 731–746, Jan. 2023, doi: 10.1007/s11269-022-03397-6.

[29] X. Fan and X. Yu, "An innovative machine learning based framework for water distribution network leakage detection and localization," *Struct. Health Monitor.*, vol. 21, no. 4, pp. 1626–1644, Aug. 2021, doi: 10.1177/14759217211040269.

[30] D. Cer, Y. Yang, S.-Y. Kong, N. Hua, N. Limtiaco, R. S. John, N. Constant, M. Guajardo-Cespedes, S. Yuan, C. Tar, Y.-H. Sung, B. Strope, and R. Kurzweil, "Universal sentence encoder," 2018, *arXiv:1803.11175*.

[31] L. C. Chen, Y. Zhu, G. Papandreou, F. Schroff, and H. Adam, "Encoder–decoder with atrous separable convolution for semantic image segmentation," in *Proc. Eur. Conf. Comput. Vis. (ECCV)*, Munich, Germany, 2018, pp. 801–818.

[32] Z. Chen, C. K. Yeo, B. S. Lee, and C. T. Lau, "Autoencoder-based network anomaly detection," in *Proc. Wireless Telecommun. Symp. (WTS)*, Apr. 2018, pp. 1–5, doi: 10.1109/WTS.2018.8363930.

[33] F. Zhuang, Z. Qi, K. Duan, D. Xi, Y. Zhu, H. Zhu, H. Xiong, and Q. He, "A comprehensive survey on transfer learning," *Proc. IEEE*, vol. 109, no. 1, pp. 43–76, Jan. 2021, doi: 10.1109/JPROC.2020.3004555.

[34] G. Michau and O. Fink, "Unsupervised transfer learning for anomaly detection: Application to complementary operating condition transfer," *Knowl.-Based Syst.*, vol. 216, Mar. 2021, Art. no. 106816, doi: 10.1016/j.knosys.2021.106816.

[35] P. Liu, C. Xu, J. Xie, M. Fu, Y. Chen, Z. Liu, and Z. Zhang, "A CNN-based transfer learning method for leakage detection of pipeline under multiple working conditions with AE signals," *Process Saf. Environ. Protection*, vol. 170, pp. 1161–1172, Feb. 2023, doi: 10.1016/j.psep.2022.12.070.

[36] S. W. Oh, D.-B. Yoon, G. J. Kim, J.-H. Bae, and H. S. Kim, "Acoustic data condensation to enhance pipeline leak detection," *Nucl. Eng. Des.*, vol. 327, pp. 198–211, Feb. 2018, doi: 10.1016/j.nucengdes.2017.12.006.

[37] W.-H. Tu and K. Chang, "Compact microstrip low-pass filter with sharp rejection," *IEEE Microw. Wireless Compon. Lett.*, vol. 15, no. 6, pp. 404–406, Jun. 2005, doi: 10.1109/LMWC.2005.850479.

[38] F. Almeida, M. Brennan, P. Joseph, S. Whitfield, S. Dray, and A. Paschoalini, "On the acoustic filtering of the pipe and sensor in a buried plastic water pipe and its effect on leak detection: An experimental investigation," *Sensors*, vol. 14, no. 3, pp. 5595–5610, Mar. 2014, doi: 10.3390/s140305595.

[39] W. Mpesha, M. Hanif Chaudhry, and S. L. Gassman, "Leak detection in pipes by frequency response method using a step excitation," *J. Hydraulic Res.*, vol. 40, no. 1, pp. 55–62, Jan. 2002, doi: 10.1080/00221680209499873.

[40] L. McInnes, J. Healy, and J. Melville, "UMAP: Uniform manifold approximation and projection for dimension reduction," 2018, *arXiv:1802.03426*.

[41] A. Diaz-Papkovich, L. Anderson-Trocmé, and S. Gravel, "A review of UMAP in population genetics," *J. Hum. Genet.*, vol. 66, no. 1, pp. 85–91, Jan. 2021, doi: 10.1038/s10038-020-00851-4.

[42] M. Vermeulen, K. Smith, K. Eremin, G. Rayner, and M. Walton, "Application of uniform manifold approximation and projection (UMAP) in spectral imaging of artworks," *Spectrochimica Acta A, Mol. Biomolecular Spectrosc.*, vol. 252, May 2021, Art. no. 119547, doi: 10.1016/j.saa.2021.119547.

[43] S. Ruder, "An overview of gradient descent optimization algorithms," 2016, *arXiv:1609.04747*.

[44] A. Daffertshofer, C. J. C. Lamoth, O. G. Meijer, and P. J. Beek, "PCA in studying coordination and variability: A tutorial," *Clin. Biomechanics*, vol. 19, no. 4, pp. 415–428, May 2004, doi: 10.1016/j.clinbiomech.2004.01.005.

[45] J. Shlens, "A tutorial on principal component analysis," 2014, *arXiv:1404.1100*.

[46] *TensorFlow Lite*. Accessed: Nov. 2019. [Online]. Available: https://www.tensorflow.org/lite/guide

SUJIN PARK received the B.S. degree in artificial intelligence and big data engineering from Daegu Catholic University, Gyeongsan-si, Gyeongbuk, Republic of Korea, in 2022, where she is currently pursuing the M.S. degree in AI and big data engineering. Her research interests include speech synthesis, machine learning/deep learning, computer vision, and anomaly detection.

DOYEOB YEO received the B.S., M.S., and Ph.D. degrees in mathematical sciences from Korea Advanced Institute of Science and Technology (KAIST), Daejeon, South Korea, in 2009, 2012, and 2017, respectively. From 2017 to 2021, he was with the Electronics and Telecommunications Research Institute, Daejeon. In 2021, he joined Korea Atomic Energy Research Institute (KAERI), where he is currently a Senior Researcher with the Nuclear System Integrity Sensing and Diagnosis Division. His research interests include generative deep learning, meta learning, and pipe leakage detection.

JI-HOON BAE (Member, IEEE) received the B.S. degree in electronic engineering from Kyungpook National University, Daegu, Republic of Korea, in 2000, and the M.S. and Ph.D. degrees in electrical engineering from Pohang University of Science and Technology, Pohang, Gyeongbuk, Republic of Korea, in 2002 and 2016, respectively. From 2002 to 2019, he was a Principal Researcher with the Electronics and Telecommunications Research Institute, Daejeon, Republic of Korea. In 2019, he joined the Department of AI and Big Data Engineering, Daegu Catholic University, Gyeongsan, Gyeongbuk, where he is currently an Assistant Professor. His research interests include deep learning, transfer learning, radar imaging, radar signal processing, and optimized techniques. He is a member of Korea Institute of Information Technology and Korea Institute of Electromagnetic Engineering and Science.